International Journal of Cognitive Computing in Engineering 1 (2020) 45–54

Contents lists available at ScienceDirect

International Journal of Cognitive Computing in Engineering

journal homepage: https://www.keaipublishing.com/en/journals/international-journal-of-cognitive-computing-in-engineering/

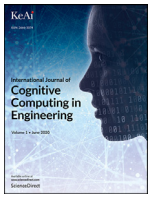

Patch-based partial motion blurred segmentation

Lin Xiang*, Xiaoling Jiang, Yueqin Xu, Yongjun Zhang, Tongqing Zhu

Huaiyin Institute of Technology, Huai'an, Jiangsu 223003, China

ARTICLE INFO

Keywords:
Local motion-blurred
Image segmentation
Patch-based segmentation

ABSTRACT

Motion blur has a significant impact on image recognition. Segmentation of motion-blurred regions contributes to further identification or classification. Most existed segmentation algorithms are always universal for partially blur images, but not especially for motion-blurred ones. This paper proposes a particular algorithm aiming at motion-blurred region segmentation. Firstly, motion regions are segmented by a patch-based preprocessing. Then, the blurriness of motion regions is measured by a defined function to detect local blurred areas. Empirical thresholds are recommended according to the experimental results. The experimental results show that the motion-blurred regions can be segmented more accurately, and the speed almost doubles other algorithms. Thus we propose a more accurate and efficient segmentation method, especially for partial motion-blurred images.

1. Introduction

In digital photography, motion blur is a common but undesirable phenomenon because it will have an impact on image recognition. It is mostly caused by the relative motion between the camera and objects (Ben-Ezra & Nayar S, 2003; Javaran et al., 2017; Li et al., 2015; Shao et al., 2015). Segmentation of blurred regions from a clear background plays an important role in subsequent image recognition or classification. This paper proposes an algorithm for detecting blurred regions and segmenting moving objects out of the non-blurred regions in images.

Many scholars have researched on blur segmentation from different perspectives. Spatial derivative (Levin, 2007; Liang et al., 2009, 2010; Marziliano et al., 2002; Ryu & Sohn, 2014; Zhang et al., 2012), the average gray level (Bar et al., 2007), the thickness of object contours (Capizzi et al., 2018; Freeman W & Adelson E, 1991; Jacob & Unser, 2004; Liu & Klette, 2017; Pi et al., 2013; Soleimani et al., 2010; Stanciu et al., 2019; Zhang & Bergholm, 1997), the color spectrum (Huang et al., 2018; Liu et al., 2008; Xu et al., 2013; Yang & Qin, 2016) are used as measurements to reflect the intensity of the blur. Besides, in the research of low-DOF (depth-of-field) images, blur segmentation is also involved (Graf et al., 2011; Kim, 2005; Li & Ngan K, 2007; Tai & Brown, 2009; Zhang K et al., 2007). Recently, more and more scholars aim at partial blur segmentation (Storath et al., 2017; Tang et al., 2016; X. Zhao & Wu, 2019, 2019). Chakrabarti et al. (2010) proposed a local blur cue to measure the likelihood of a small neighborhood being blurred by a candidate blur kernel. Combining with color information under the Markov Random Field segmentation framework, reasonable segmentation of the blurred objects were obtained. Levin Levin et al., (2008) introduced the spectral matting technique to decompose a color image into the foreground/ background. Zhao et al. (Zhao et al., 2013) combined some blur features such as gradient histogram span, local mean square error map, and maximum saturation et al. to detect the blur and appeal to image matting technology for segmentation. By overcoming the drawbacks in Zhao et al., (2013) of the needed manual intervention and unstable features, Su et al. (Su et al., 2011) used a threshold method to segment the sharp area from the blur area. Wang (Wang et al., 2014) applied morphological technologies to segment the partial blur from a single image, considering different types of blur. They also defined a criterion for ranking the blur degree of a partial blur image. Kovacs and Szirnyi (Kovacs & Sziranyi, 2007) differentiate the blurred areas by deconvolution-based focus extraction with the angle deviation error measure in blind image deconvolution. Besides Taiebeh et al. (Javaran T et al., 2016) proposed the noise-immune blur metric for blur estimation, by which the blurriness values of divided blocks were calculated. Taiebeh et al. (Javaran T et al., 2017) also encoded the amount of blurriness for individual pixels in a given image to detect blurred regions.

Summing up all the above-mentioned work, we find that most segmentation algorithms are fit for universal partial blur images but not especially for motion-blur. The way of estimating the blur kernel to deal with motion blur always results in discontinuities, while measuring local blurred region pixel to pixel is accurate but time-consuming. This paper proposed a local segmentation algorithm, especially for motion blur. The main contributions of this paper are: (1) to pre-segment the image in a patch-based way to detect the motion regions; (2) to mea-

* Corresponding author.
E-mail address: wllgnxl99@163.com (L. Xiang).

https://doi.org/10.1016/j.ijcce.2020.10.001
Received 20 March 2020; Received in revised form 16 October 2020; Accepted 16 October 2020
Available online 18 October 2020

sure the blurriness of patches to segment blurred regions; (3) to provide empirical values of the thresholds.

The rest of this paper is organized as follows. Section 2 and 3 describe the two stages of the proposed motion blur segmentation algorithm. The experimental results and discussions are presented in Section 4. Finally, we summarize and discuss directions for future research in Section 5.

2. Patch-based pre-segmentation

Image segmentation is a technique to divide an image into several regions with specific meanings, according to different features, such as grayscale, texture. Each region has the same or similar feature, different from other regions. Thus the image segmentation can be seen as a process of classifying pixels according to certain criteria is essential. Under the concept of the set, image segmentation can be defined as:

Definition 1. Let the set of all the pixels in a digital image I be R, P be the logical predicate (Classification criteria), then image segmentation is to divide R into N subsets $\{S_1, S_2, \cdots, S_N\}$, which meet:

(1) $\bigcup_{i=1}^{N} S_i = R$;
(2) $S_i \cap S_j = \Phi, \quad i \neq j$;
(3) $P(S_j) = \text{TRUE}$;
(4) $\forall i \neq j, P(S_i \cup S_j) = \text{FALSE}$;
(5) Each S_i is a connected region.

The condition(2) denotes that each sub-region in the segmentation result does not overlap with others. (3) means that similar features exist in the same sub-region and (4) means that different subdomains describe different features. From the above definition, the key to image segmentation is to find specified features as criteria for the classification of pixels. As far as the partial motion blur images are concerned, the most significant features are motion and blur for the relative motion during the moment of exposure. A targeted algorithm is then proposed for this kind of segmentation.

2.1. Orientation of the patch

At the moment of exposure, large quantities of straight lines in almost the same direction are generated in local regions of moving objects. The massive lines have a great impact on the orientation of the whole image. Intuitively, the gradient can be taken as a measure for the orientation of the pixel and the pixels with almost the same orientation compose the motion regions. However, it is too time-consuming. In fact, pixels in the motion regions are almost in the same direction as the patch. Thus it is more practical to determine the rough orientation of the patch or the image, instead of calculating the orientations of each pixel. Therefore we divide the image into patches and make a definition of the orientation of each patch.

Definition 2. Let I be a patch of an image, $\nabla I = [\nabla I_x, \nabla I_y]$be the gradient of the patch I, $SG_x$and $SG_y$are the components of the squared gradient vector of the patch in x-direction and y-direction respectively. Then the orientation of the patch OI is defined as follows:

$$OI = SG_x / SG_y \tag{1}$$

where $SG_x = \nabla I_x^2$and $SG_y = \nabla I_y^2$.

From the formula(1), the orientation of each patch with that of the image can both be found. Compared with the orientation of the whole image, the patches in nearly the same orientation are considered to be motion regions. By setting a proper threshold α_0, the patches with directions fluctuating around the orientation of the whole image in a range of the threshold are seemed as motion-blurred. Thus the rough segmentation can be done to trace the motion regions caused by the moving of the objects. In practical, for the convenience of setting threshold, the orientation can be represented as an angle:

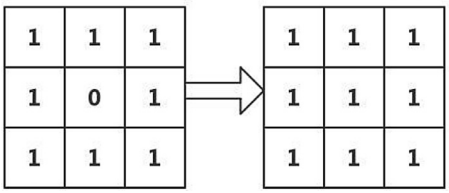

Fig. 1. The operation of assimilation.

$$\alpha = arctan(OI) \tag{2}$$

where α is the corresponding angle of $OI$and $arctan(\cdot)$is the arctangent function.

After the segmentation, the motion regions in almost the same direction can be roughly located. However, lines in the background, such as zebra crossings or driving lines will be mis-contained in the segmented regions, because these kinds of lines also have directions. Further segmentation on the rough results is needed to eliminate the backgrounds not belonging to motion-blurred regions.

2.2. Assimilation

Based on the above method, motion regions can be separated but with some isolated points with different directions from the surrounding pixels, which leads to the undesired discontinuous segmented regions. In order to solve the problem of discontinuity of image patches, this paper proposes a method based on the blurriness map to remove the isolated points by comparing the relationship between outliers and adjacent regions according to some assimilating rules. Firstly, we construct the blurriness map based on the results of the previous results. That is to binarize the segmented image by marking the areas with 1 that are in almost the same direction as the moving objects while marking the other areas with 0. Assimilation is to consider the effect of the surrounding pixels around a certain pixel in the blurriness map. Taking a range with the size of 3×3 as considering, as shown in Fig. 1, nine elements of 0 or 1 in the range are summed up. If the sum is greater than 5 and the element is 0, we change the value of the element and remark it with 1. In this way, the whole blurriness map matrix is traversed to realize the operation of assimilation. After the traversal on the whole map, the isolated points in different directions from most of the pixels in the regions can be removed. Consequently, continuous regions are obtained to facilitate further segmentation.

3. Segmentation based on blurriness measurement

The above-segmented results contain not only motion regions but also backgrounds in the same direction as the moving objects, such as zebra crossings or fences on the road. So the next step is to segment these non-ambiguous but directional regions. The key of this step is to define and evaluate the blurriness according to a certain principle and then set suitable thresholds for distinguishing the blur and non-blur. Motion blurring is aroused by the superposition of pixels because of the relative motion at the moment of exposure. Therefore, we need to evaluate the blurring degree and give an objective evaluation criterion. Further segmentation can be continued according to the criterion to obtain the target blurred areas.

However, most existed methods can only evaluate the fuzzy degree of the global but not local regions. To segment motion-blurred regions under a clear background, a unified standard should be designed to measure the blurriness of different regions in the whole image. Therefore, an evaluating function is proposed in this paper to measure the severity of blurring.

As one kind of subjective feeling, blurring is the most intuitive reflection of the change of gray values to human eyes. Generally, to digital images, slow changes of the gray values present blurriness to some extent. Nevertheless, it does not mean that the more slowly gray values change, the region is more blurry. Some areas are not blurred although the gray values in these areas change slowly, such as the sky, road, and other gentle areas. Theoretically, gray values of blurred regions should change more gently than marginal areas, but more sharply than regions in which gray values hardly change. Based on the above analysis, we define a function to measure the blurriness of regions by which the function values of the blurred regions can be maximized.

Definition 3. Let I be a patch of an image, ∇^2be the squared gradient of the patch I, then the blurriness function is defined as λ:

$$\lambda = \gamma_1 exp(-(\nabla^2 - \mu)^2/\sigma^2) + \gamma_2 \tag{3}$$

where $\gamma_1$and $\gamma_2$are constants in [0,1]. By setting the values of $\gamma_1$and γ_2, the range of the above blurriness function is refined in 0 to 1. $\mu$is the mean of squared gradients, and $\sigma$is the standard deviation of the patch.

$$\mu = \frac{1}{n}\sum_{i=1}^{n}\nabla^2,\ \sigma = \sqrt{\frac{1}{n-1}\sum_{i=1}^{n}(\nabla^2 - \mu)^2} \tag{4}$$

n is the number of pixels in the patch. By the defined function, when the gradient of the squares of the patch $\nabla^2$is too large or too small, the corresponding function value approaches to zero. Instead in the middle region, the corresponding function value is maximized.

The squared gradient can measure the variation of the pixel values around a point in the image. So, the sum of the squared gradient∇^2reflects the change of the pixels in the patch. $\nabla^2$is much bigger in margin area because gray values change so sharp but smaller in regions like grounds and walls with little changes. In fact, ∇^2blurred regions should be between the large and the small, near to the mean. According to the definition, while$\nabla^2$is in the middle region, the maximum of the function is reached to represent the most blurry regions in the image, which just meet our expectation. By setting a proper threshold λ_0, the sub-blocks whose blurriness function values exceed $\lambda_0$can be considered to be blurred regions. Thus combined with the pre-segmented results in the previous stage, the partial motion-blurred regions can be split out by now. Fig. 2 shows the whole segmentation flow.

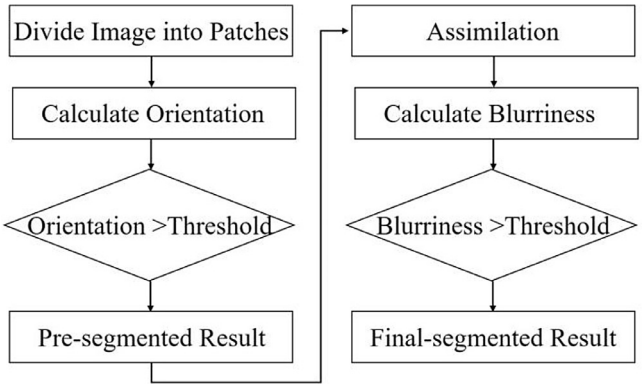

Fig. 2. Flow of the motion blur segmentation algorithm.

4. Experiments and results

In this section, a series of experiments are run on the public data set Blur Detection Dataset (Liu et al., 2008) (BDD) to verify the effectiveness of the proposed algorithm in this paper. This dataset contains 1050 blurred and sharp images (350 triplets), each image triplet is a set of three photos of the same scene: sharp, defocused-blurred, and motion-blurred images. In addition, we also collect 1000 images containing partial motion-blurred objects in different scenarios, including streets, parking lots, inter-mountains, and wilds. The hardware configurations of the computer used in the experiments are Intel(R) Core(TM) i5–4210 M CPU @ 2.60 GHz, 8GB RAM.

4.1. Experiment I

In the two stages of the segmentation algorithm, there are 3 key thresholds: the size of the patch l, the orientation angle α_0, and the threshold of blurriness λ_0. By fixing one threshold and adjusting the others, we choose appropriate threshold parameters by testing experiments.

In the first series of experiments, we test the effects of different thresholds of patch size l on the pre-segmented results.Under a fixed threshold $\alpha_0 = 25^{\cdot}$, the patch sizes are set to five different values: $l = 10,30,50,70,90$. Fig. 3 shows the segmented results of a sample image in the BDD set in different patch sizes. It is easy to see that the result is the best when l is 50. With the same fixed thresholds $\alpha_0$and l, the other

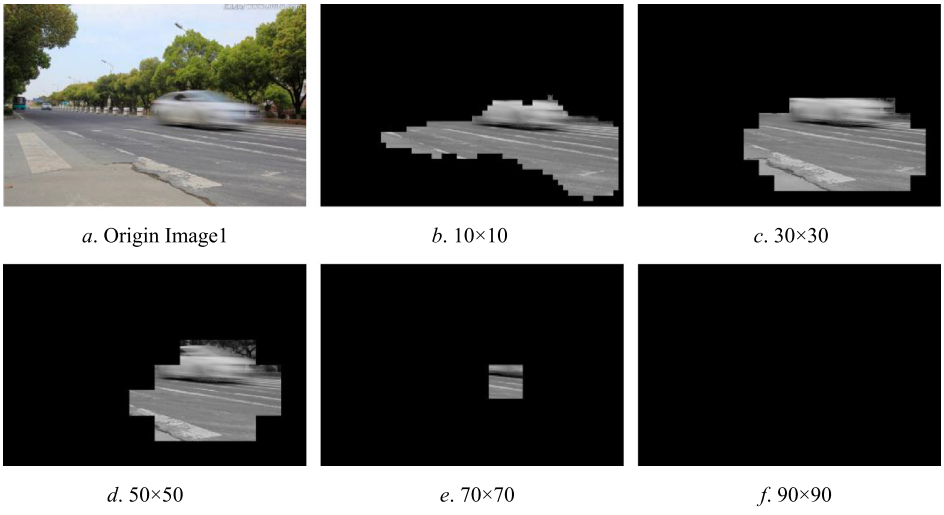

a. Origin Image1 *b*. 10×10 *c*. 30×30

d. 50×50 *e*. 70×70 *f*. 90×90

Fig. 3. The origin image and the segmented images with different patch size.

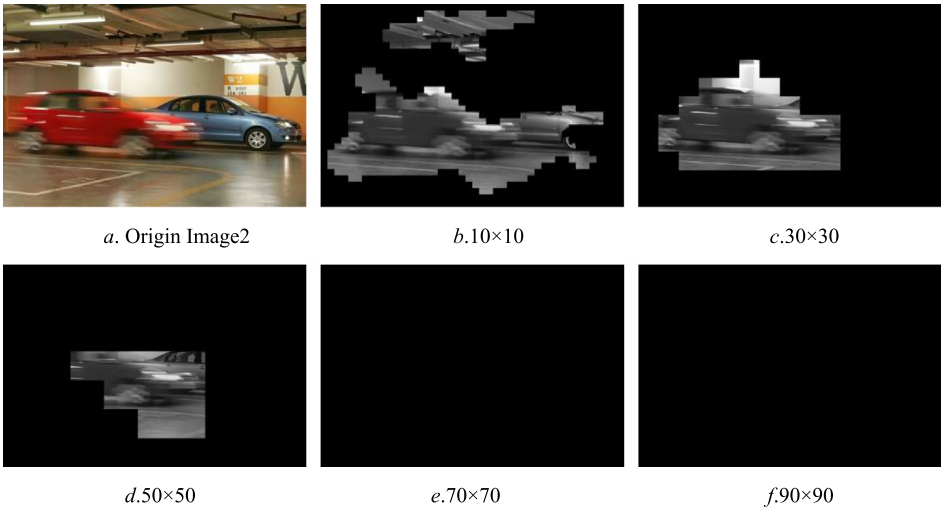

a. Origin Image2 *b*.10×10 *c*.30×30

d.50×50 *e*.70×70 *f*.90×90

Fig. 4. The origin image and the segmented images with different patch size.

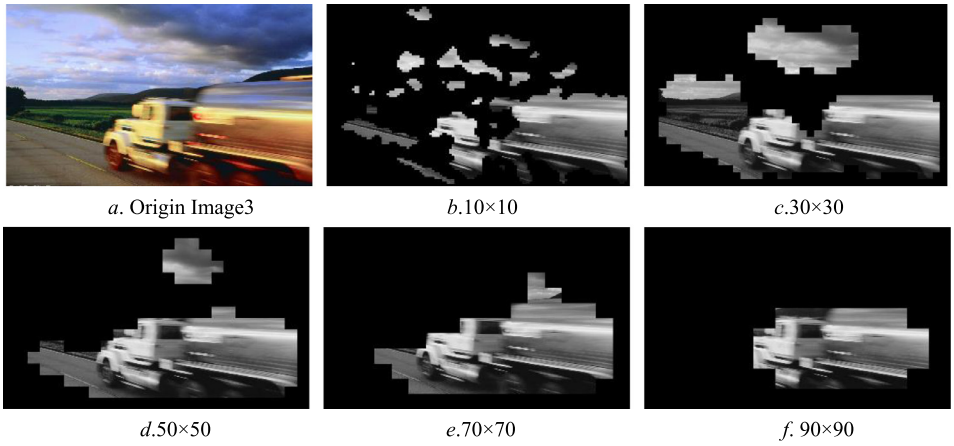

a. Origin Image3 *b*.10×10 *c*.30×30

d.50×50 *e*.70×70 *f*. 90×90

Fig. 5. The origin image and the segmented images with different patch size.

two images are tested, as shown in Figs. 4 and 5. It can be seen that when the patch size is set to 30 and 90 for the two images respectively, the corresponding results achieve the best.

Similar tests on the data set show that it is hard to achieve ideal results whatever the patch size is too large or too small. Actually, the patch size determines the accuracy of the segmentation. While the patch is larger, the segmentation is too rough to obtain the detailed features of the patch. In extreme cases, none regions exist after segmentation, such as in Figs. 3(*f*), 4(*e*), and 4(*f*) by setting too large size compared to the size of the original image. On the contrary, the segmentation with a smaller size of patches will generate more precise results. However, it is meanwhile time-consuming and causing some irrelevant regions in the backgrounds, as shown in Figs. 3(*b*) -5(*b*) with the size value of $l = 10$. Through multiple experiments, we find that 10% of the original image size is the best proper threshold of the patch size l.

In the same way, different orientation angles are tested by setting $\alpha_0 = 5^{\circ},15^{\circ},25^{\circ},35^{\circ},45^{\circ}$ with the fixed threshold $l$of 10% the original image size. Figs. 6–8 shows the pre-segmented results of the portion of samples in the image dataset under the different thresholds α_0. $\alpha_0$represents the deviation from the overall direction of the image. While $\alpha_0$is too small, only minor deviations are allowed and few regions can be retained. Taking 5° to be concerned, hardly regions are left behind after pre-segmentation as shown in Figs. 6(*b*)–8(*b*). Theoretically, the bigger $\alpha_0$is, the more regions can be contained. However too big deviation will result in the inclusion of too many irrelevant areas as shown in Fig. 8(*f*). By comparison, α_0=25° is a relatively proper value for good results. l and $\alpha_0$are the crucial thresholds during the process of pre-segmentation, which will greatly affect the successive segmentation.

After setting proper thresholds of l and α_0, the pre-segmentation can be realized by which rough regions contain massive straight lines that can be split out first. Then we test the effects of the threshold $\lambda_0$for further segmentation. With proper values of $l = 40$ and α_0=25°, a series of values $\lambda_0$are set for testing ranging from 0.1 to 0.9 with a step of 0.2. $\lambda_0$is used to measure the blurriness of the patch. According to the properties of the defined blurriness function, the function values corresponding to near the mean of the arguments $\nabla^2$are larger, while smaller when $\nabla^2$is too large or too small. Patches with larger blurriness function values than $\lambda_0$are taken as the blurred regions. Figs. 9–11 shows the segmentation results of partial sample images in the image set according to different values λ_0. It can be seen that too small or too large $\lambda_0$results in undesirable results. Theoretically, it is suitable to set $\lambda_0$as the value near the function value corresponding to the mean value of squared gradients of all patches in the image. Empirically, 0.7 is a recommended value for the blurriness threshold λ_0.

Furthermore, we verify the effectiveness of the algorithm in the various cases with different backgrounds and speeds of motions, especially for slowly moving objects. Fig. 12 shows the segmented result by our method on Image 4 to Image 8. Image 4 and Image 5 show the case of moving objects at high speed for which many lines are caused. It can be seen that the results are satisfactory with almost complete segmenta-

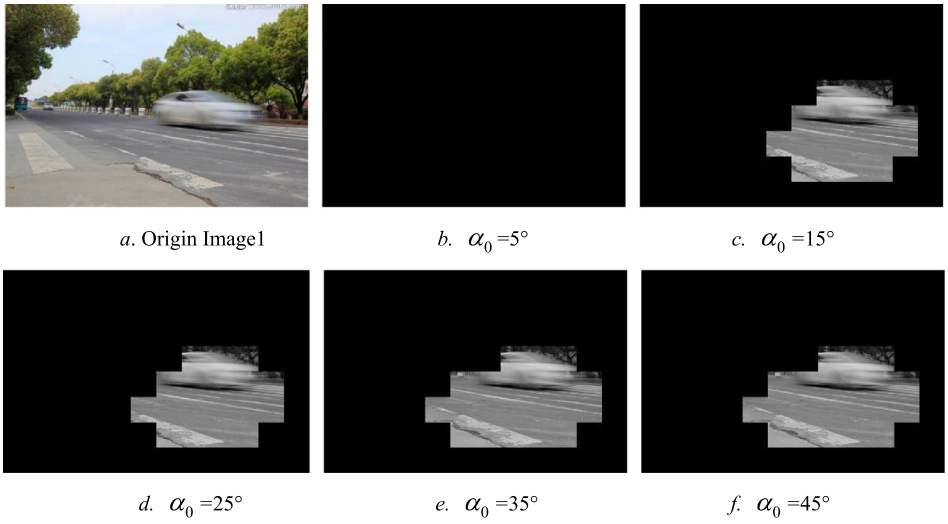

a. Origin Image1 *b*. α_0 =5° *c*. α_0 =15°

d. α_0 =25° *e*. α_0 =35° *f*. α_0 =45°

Fig. 6. The origin image and the segmented images with different α_0.

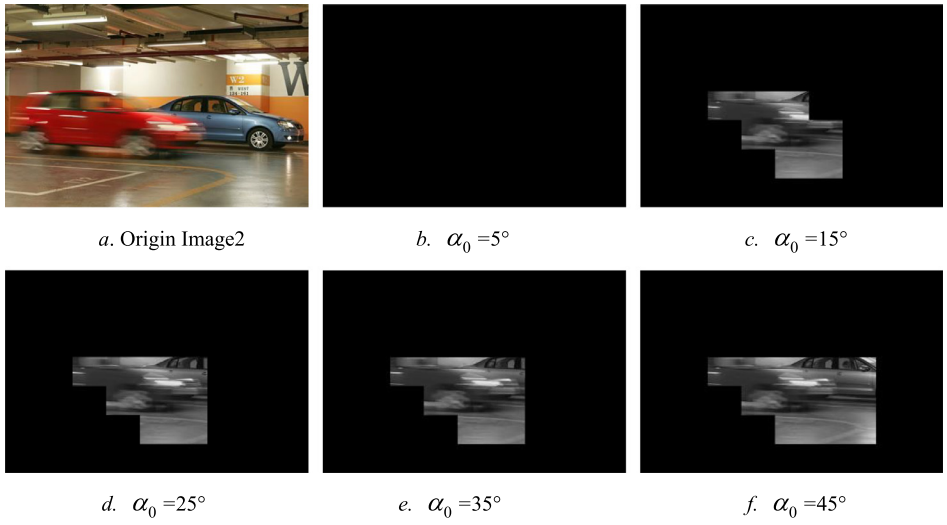

a. Origin Image2 *b*. α_0 =5° *c*. α_0 =15°

d. α_0 =25° *e*. α_0 =35° *f*. α_0 =45°

Fig. 7. The origin image and the segmented images with different α_0.

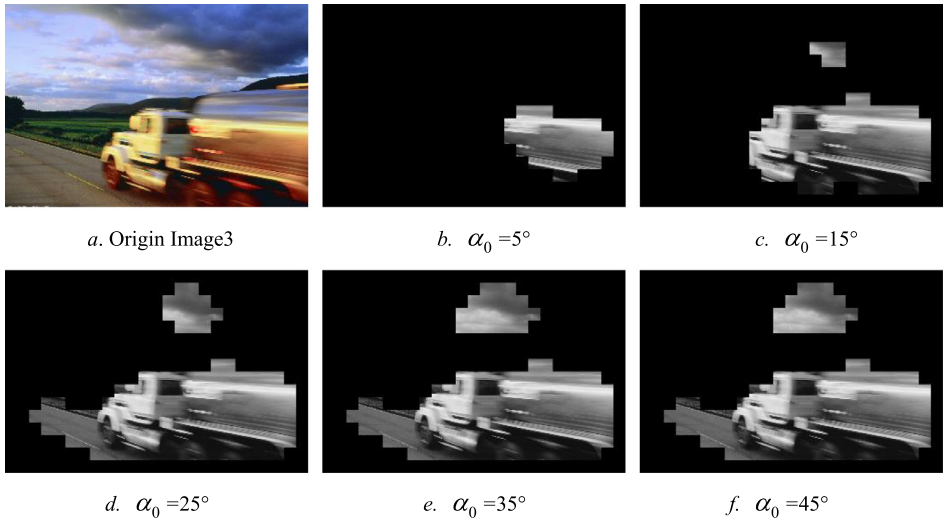

a. Origin Image3 *b*. α_0 =5° *c*. α_0 =15°

d. α_0 =25° *e*. α_0 =35° *f*. α_0 =45°

Fig. 8. The origin image and the segmented images with different α_0.

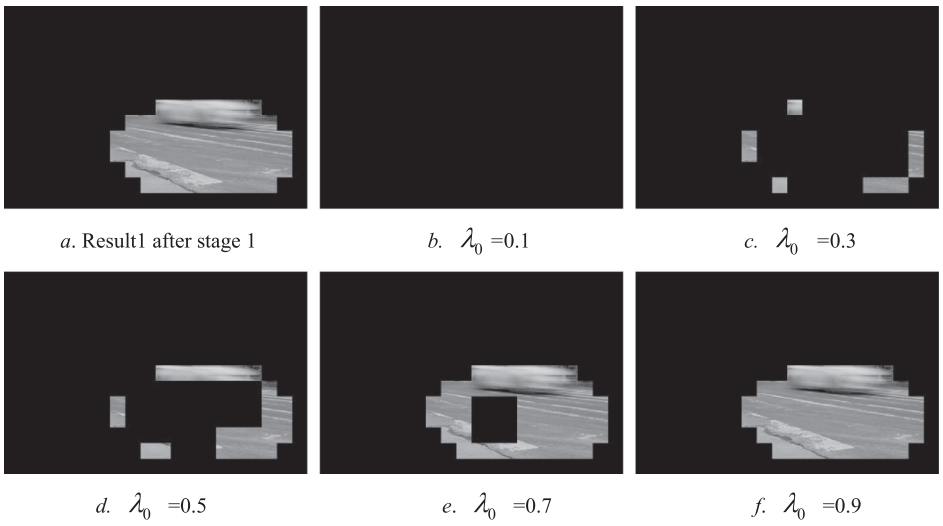

Fig. 9. The segmented result after stage 1 and further results with differentλ_0.

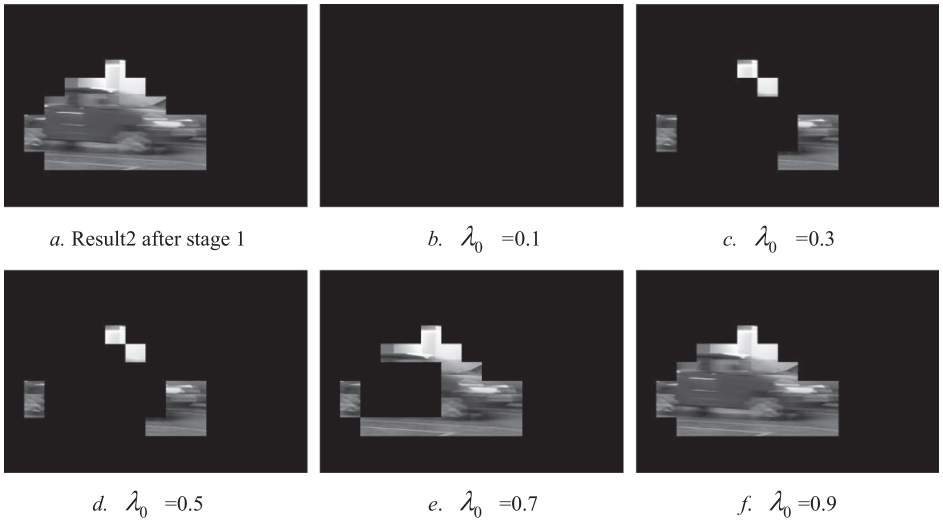

Fig. 10. The segmented result after stage 1 and further results with differentλ_0.

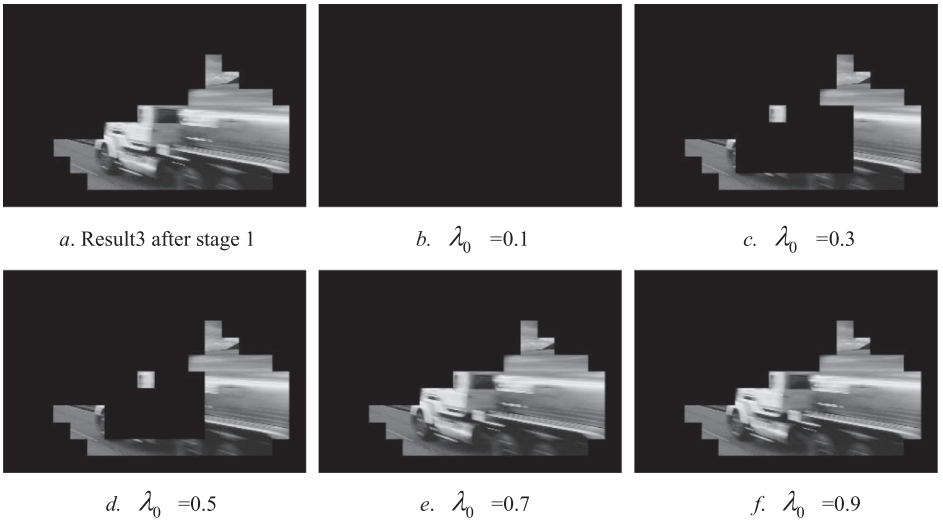

Fig. 11. The segmented result after stage 1 and further results with differentλ_0.

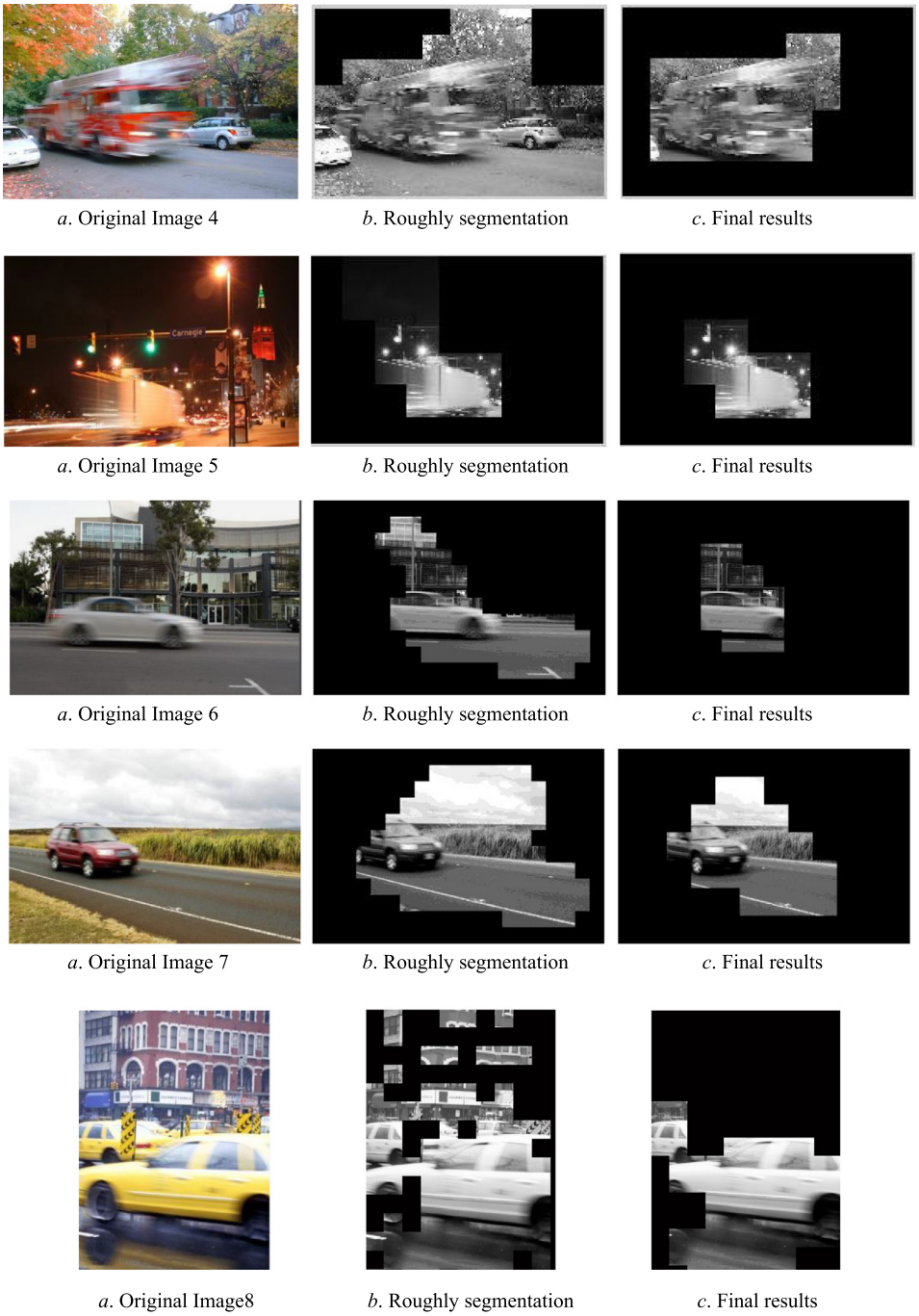

Fig. 12. Results with different backgrounds and speeds.

tion of moving cars. By contrast, Image 6–8 are the cases of motion blur with low speed and complex backgrounds. Taking Image 8 for example, a moving taxi with very low speed generates hardly straight lines which have little effect on the overall direction. Meanwhile, some clean-cut buildings exist in the backgrounds. It is not conducive to both the two aspects of the implementation of the proposed segmentation algorithm. Rough results show the pre-segmentation based on the orientation. It can be seen that some edges of buildings in the backgrounds are included in the result. However, those undesired backgrounds are eliminated by the blurriness function in the successive segmentation as shown in the final results. Similarly acceptable results are shown in other sample images(Image 6 and Image 7). Therefore, it is also feasible of our proposed algorithm for the segmentation of motion-blurred objects at low speed, even in the extreme case that directional edges exist in the backgrounds simultaneously. In summary, our algorithm is valid for the partial motion-blurred segmentation. Comparatively, objects at the high speed are apt to be split because of its clear moving traces during the motion.

4.2. Experiment II

To verify the feasibility of the proposed algorithm, we compare the results with the algorithms in Su et al., (2011) and Jin-ming et al., (2014). (Su et al., 2011) classifies the types of blurred images into a defocus blur and motion blur by analyzing the information of channel α. They developed a criterion for measuring the blurriness and used

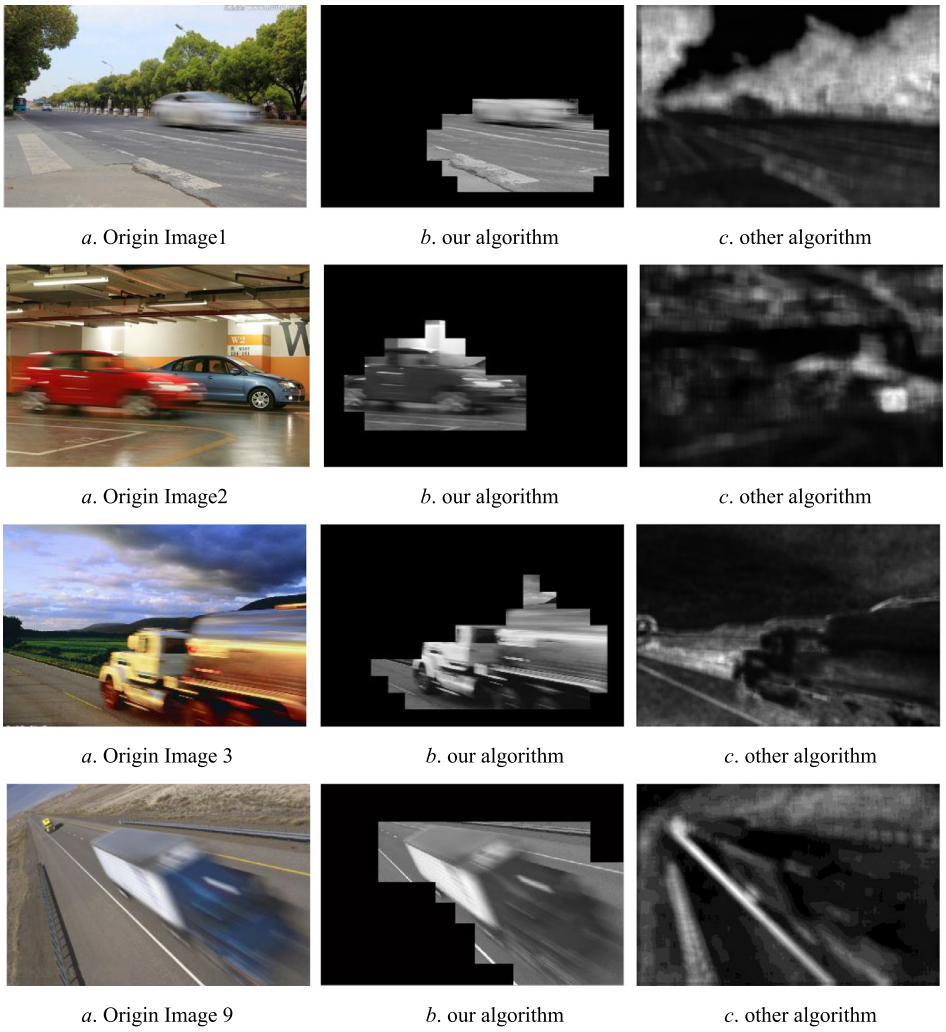

Fig. 13. Compared results of our algorithm with the other algorithm (Su et al., 2011).

singular value to segment the blurred regions. Fig. 13 shows the segmented results of various images by the proposed algorithm in this paper with the one in Su et al., (2011). The middle of the four arrays of images correspond to the results of our proposed algorithm, while the right are the results of the algorithm in Su et al., (2011). It can be seen that the algorithm in Su et al., (2011) is almost invalid for this kind of blurriness. Comparatively, the proposed algorithm in this paper is designed according to the two typical characteristics of this kind of blur: (1) massive straight lines in almost the same direction exist for the motion of objects during the exposure; (2) partial overlapping blur is contained for the relative motion of the moving objects with the camera. Aiming at the two aspects, we first roughly split the image into patches to segment motion regions according to orientation angles, which is caused by massive straight lines. And then the intensity of blur is measured by the defined function for further segmentation of blurred regions. The experimental results show that this targeted design mechanism achieves a better segmentation effect.

In addition, we compare our method with (Jin-ming et al., 2014). (Jin-ming et al., 2014) adds Gaussian noise into image patches to re-blur the original image and then consider the change of singular values before and after the noise addition to determine the patch is blur or not. Fig. 14 shows the segmented result by our algorithm and (Jin-ming et al., 2014). It is not hard to see that the segmented results by our method are better than the other algorithm. The partial motion-blurred regions are almost split out of the background. In most cases, motion blur occurs on the cars in the street, so we choose four arrays of images with moving cars as samples. Racing lines on the road or lines on the grounds of the parking always greatly affect the segmentation. By the proposed algorithm, lines on the grounds in the same direction as the moving car are almost removed, especially in the bottom three arrays of images. Thus as far as the segmentation results are concerned, our algorithm is more suitable for the blur regions segmentation which is caused by objects' moving. To be further, the singular value based algorithm is realized in the mode of pixel to pixel, which is a bit time-consuming. In comparison, the proposed patch-based algorithm in this paper is more efficient in dealing with these tasks, which is run in the unit of the patch but not the pixel. It is found that the segmenting speed by our algorithm is almost double the algorithm of the other one. Thus we offer a feasible and efficient method for motion blurred segmentation.

5. Conclusion

Motion blur is very common in life such as in traffic surveillance video, and the targeted solution is of great help to further recognition or retrieval. This paper focuses on the blurred image segmentation which is caused by object motions. Considering the typical char-

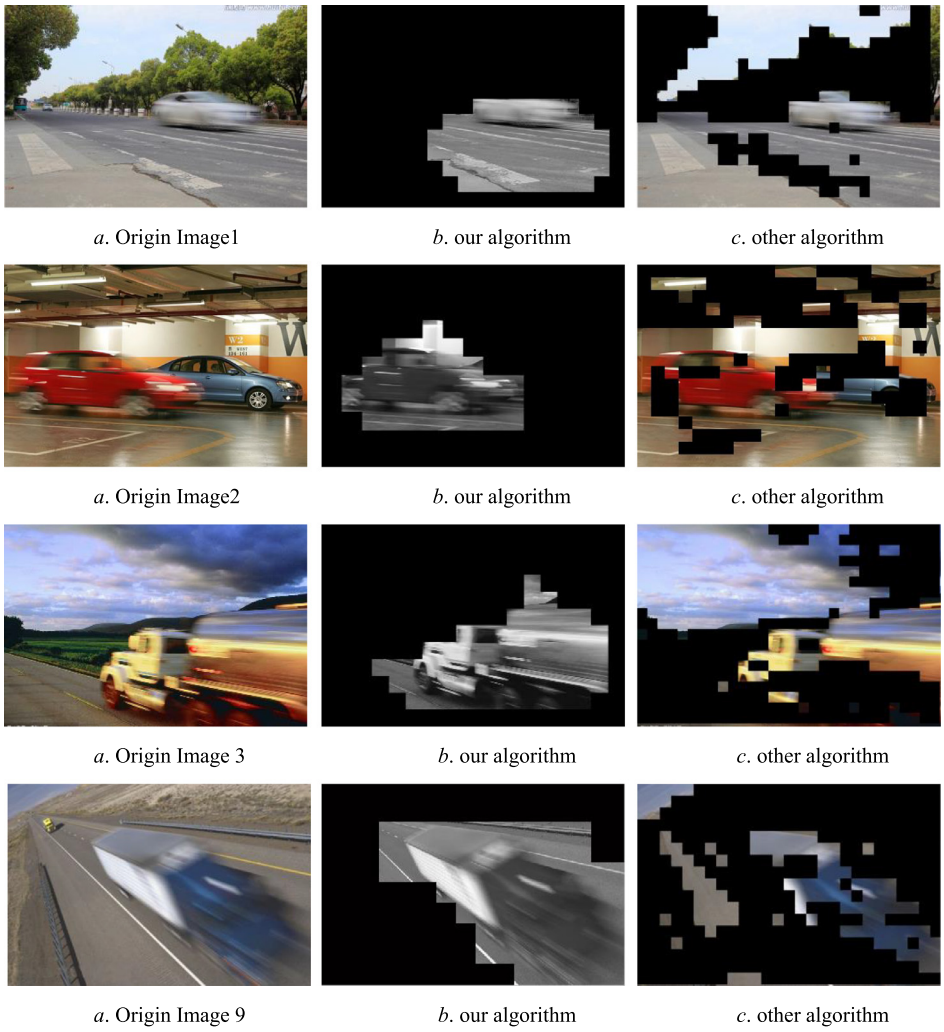

Fig. 14. Compared results of our algorithm with the other algorithm (Jin-ming et al., 2014).

acteristics of this kind of blur, a patch-based algorithm is proposed and realized in two stages: pre-segmentation by orientations and further segmentation by measuring the blurriness. Proper threshold values are recommended empirically. Experimental results verify the feasibility of the proposed method and it outperforms other existing approaches both on the effects and the speed. Moreover, the algorithm also works even under adverse conditions. Thus we put forward a feasible and efficient method especially toward the issue of the partially motion-blurred segmentation. In the future, we will research on the automatic setting of parameters and other partially blurred segmentation.

Declaration of Competing Interests

The authors declare that they have no known competing financial interests or personal relationships that could have appeared to influence the work reported in this paper.

Acknowledgments

This work is supported by Science Research Project of Huaiyin Institute of Technology under Grant No. Z201A19507.

References

Bar, L., Sochen, N., & Kiryati, N. (2007). Restoration of images with piecewise space-variant blur. In *International conference on scale space and variational methods in computer vision* (pp. 533–544). Springer.

Ben-Ezra, M., & Nayar S, K. (2003). Motion deblurring using hybrid imaging. In *2003 IEEE computer society conference on computer vision and pattern recognition. Proceedings: 1*. IEEE I-I.

Capizzi, G., Coco, S., Sciuto G, L., et al. (2018). A new iterative FIR filter design approach using a Gaussian approximation[J]. *IEEE Signal Processing Letters, 25*(11), 1615–1619.

Chakrabarti, A., Zickler, T., & Freeman W, T. (2010). Analyzing spatially-varying blur. In *2010 IEEE Computer Society Conference on Computer Vision and Pattern Recognition* (pp. 2512–2519). IEEE.

Freeman W, T., & Adelson E, H. (1991). The design and use of steerable filters. *IEEE Transactions on Pattern Analysis & Machine Intelligence, 1991*(9), 891–906.

Graf, F., Kriegel H, P., & Weiler, M. (2011). Robust segmentation of relevant regions in low depth of field images. In *2011 18th IEEE international conference on image processing* (pp. 2861–2864). IEEE.

Huang, R., Feng, W., Fan, M., et al. (2018). Multiscale blur detection by learning discriminative deep features. *Neurocomputing, 285*, 154–166.

Jacob, M., & Unser, M. (2004). Design of steerable filters for feature detection using canny-like criteria. *IEEE transactions on pattern analysis and machine intelligence, 26*(8), 1007–1019.

Javaran T, A., Hassanpour, H., & Abolghasemi, V. (2016). A noise-immune no-reference metric for estimating blurriness value of an image. *Signal Processing: Image Communication, 47*, 218–228.

Javaran T, A., Hassanpour, H., & Abolghasemi, V. (2017). Automatic estimation and segmentation of partial blur in natural images. *The Visual Computer, 33*(2), 151–161.

Javaran, T. A., Hassanpour, H., & Abolghasemi, V. (2017). Local motion deblurring using an effective image prior based on both the first-and second-order gradients. *Machine Vision and Applications, 28*(3–4), 431–444.

Jin-ming, G., Zhao-yong, X., Zhen-ming Y, U., et al. (2014). An image blurred region

detection and segmentation new method using singular value decomposition. *Journal of Signal Processing, 30*(5), 569–574.
Kim, C. (2005). Segmenting a low-depth-of-field image using morphological filters and region merging. *IEEE Transactions on Image Processing, 14*(10), 1503–1511.
Kovacs, L., & Sziranyi, T. (2007). Focus area extraction by blind deconvolution for defining regions of interest. *IEEE transactions on pattern analysis and machine intelligence, 29*(6), 1080–1085.
Levin, A. (2007). Blind motion deblurring using image statistics. In *Advances in neural information processing systems* (pp. 841–848).
Levin, A., Rav-Acha, A., & Lischinski, D. (2008). Spectral matting. *IEEE Transactions on Pattern Analysis and Machine Intelligence, 30*(10), 1699–1712.
Li, H., & Ngan K, N. (2007). Unsupervized video segmentation with low depth of field. *IEEE Transactions on Circuits and Systems for Video Technology, 17*(12), 1742–1751.
Li, H., Zhang, Y., & Sun, J. (2015). Motion deblurring using the similarity of the multi-scales. *Optik, 126*(4), 473–477.
Liang, L., Chen, J., & Ma, S. (2009). A no-reference perceptual blur metric using histogram of gradient profile sharpness. In *2009 16th IEEE international conference on image processing (ICIP)* (pp. 4369–4372). IEEE.
Liang, L., Wang, S., & Chen, J. (2010). No-reference perceptual image quality metric using gradient profiles for JPEG2000. *Signal Processing: Image Communication, 25*(7), 502–516.
Liu, D., & Klette, R. (2017). Blur estimation for natural edge appearance in computational photography. In *Pacific-Rim symposium on image and video technology* (pp. 300–310). Cham: Springer.
Liu, R., Li, Z., & Jia, J. (2008). Image partial blur detection and classification. In *2008 IEEE conference on computer vision and pattern recognition* (pp. 1–8). IEEE.
Marziliano, P., Dufaux, F., Winkler, S., et al. (2002). A no-reference perceptual blur metric. In *Proceedings. International conference on image processing: 3*. IEEE III-III.
Pi, F., Zhang, Y., Lu, G., et al. (2013). Defocus blur estimation from multi-scale gradients. *Fifth international conference on machine vision (ICMV 2012): Computer vision, image analysis and processing. international society for optics and photonics*: 8783.
Ryu, S., & Sohn, K. (2014). No-reference perceptual blur model based on inherent sharpness. In *2014 IEEE international conference on image processing (ICIP)* (pp. 580–584). IEEE.
Shao, W. Z., Ge, Q., Deng H, S., et al. (2015). Motion deblurring using non-stationary image modeling. *Journal of Mathematical Imaging and Vision, 52*(2), 234–248.
Soleimani, S., Rooms, F., Philips, W., et al. (2010). Image fusion using blur estimation. In *2010 IEEE international conference on image processing* (pp. 4397–4400). IEEE.
Stanciu, L., Stanciu, V., & Badea, R. (2019). Digital crossover filters designed by using B-spline functions. In *2019 international symposium on signals, circuits and systems (ISSCS)* (pp. 1–4). IEEE.
Storath, M., Rickert, D., & Unser, M. (2017). Fast segmentation from blurred data in 3D fluorescence microscopy. *IEEE Transactions on Image Processing, 26*(10), 4856–4870.
Su, B., Lu, S., & Tan C, L. (2011). Blurred image region detection and classification. In *Proceedings of the 19th ACM international conference on Multimedia: 2011* (pp. 1397–1400).
Tai, Y. W., & Brown, M. S. (2009). Single image defocus map estimation using local contrast prior. In *Image processing (ICIP), 2009 16th IEEE international conference* (pp. 1797–1800).
Tang, C., Wu, J., & Hou, Y. (2016). A spectral and spatial approach of coarse-to-fine blurred image region detection. *IEEE Signal Processing Letters, 23*(11), 1652–1656.
Wang, W., Zheng, J., & Zhou, H. (2014). Segmenting, removing and ranking partial blur. *Signal, Image and Video Processing, 8*(4), 647–655.
Xu, W., Mulligan, J., Xu, D., et al. (2013). Detecting and classifying blurred image regions. In *2013 IEEE international conference on multimedia and expo (ICME)* (pp. 1–6). IEEE.
Yang, D., & Qin, S. (2016). Restoration of partial blurred image based on blur detection and classification. *Journal of Electrical and Computer Engineering, 2016*, 1.
Zhang K, D., Lu H, Q., Wang Z, Y., et al. (2007). A fuzzy segmentation of salient region of interest in low depth of field image. In *International conference on multimedia modeling* (pp. 782–791). Springer.
Zhang, L., Zhang, L., & Mou, X. (2012). A comprehensive evaluation of full reference image quality assessment algorithms. In *2012 19th IEEE international conference on image processing* (pp. 1477–1480). IEEE.
Zhang, W., & Bergholm, F. (1997). Multi-scale blur estimation and edge type classification for scene analysis. *International Journal of Computer Vision, 24*(3), 219–250.
Zhao, J., Feng, H., Xu, Z., et al. (2013). Automatic blur region segmentation approach using image matting. *Signal, Image and Video Processing, 7*(6), 1173–1181.
Zhao, X., & Wu, Y. (2019a). Automatic motion-blurred hand matting for human soft segmentation in videos. In *International conference on image processing* (pp. 1450–1454).
Zhao, X., & Wu, Y. (2019b). Automatically extract semi-transparent motion-blurred hand from a single image. *IEEE Signal Processing Letters, 26*(11), 1598–1602.